Effects of the Discharge Parameters on the Efficiency and Stability of Ambient Metastable-Induced Desorption Ionization

2015 Plasma Sci. Technol. 17 1048

(http://iopscience.iop.org/1009-0630/17/12/1048)

Effects of the Discharge Parameters on the Efficiency and Stability of Ambient Metastable-Induced Desorption Ionization*

ZHANG Xiaotian (张晓天)[1,2], CHEN Chilai (陈池来)[1], LIU Youjiang (刘友江)[1,3], WANG Hongwei (王泓伟)[1,3], ZHANG Lehua (张乐华)[1,3], KONG Deyi (孔德义)[1], Mario CHAVARRIA[4]

[1]State Key Laboratory of Transducer Technology, Hefei Institute of Intelligent Machines, CAS, Hefei 230031, China
[2]College of Electronic Science and Applied Physics, University of Technology, Hefei 230011, China
[3]Department of Automation, University of Science and Technology of China, Hefei 230027,China
[4]Microsystems Laboratory, Ecole Polytechnique Fédérale de Lausanne (EPFL), CH-1015 Lausanne, Switzerland

Abstract Ionization efficiency is an important factor for ion sources in mass spectrometry and ion mobility spectrometry. Using helium as the discharge gas, acetone as the sample, and high-field asymmetric ion mobility spectrometry (FAIMS) as the ion detection method, this work investigates in detail the effects of discharge parameters on the efficiency of ambient metastable-induced desorption ionization (AMDI) at atmospheric pressure. The results indicate that the discharge power and gas flow rate are both significantly correlated with the ionization efficiency. Specifically, an increase in the applied discharge power leads to a rapid increase in the ionization efficiency, which gradually reaches equilibrium due to ion saturation. Moreover, when the discharge voltage is fixed at 2.1 kV, a maximum efficiency can be achieved at the flow rate of 9.0 m/s. This study provides a foundation for the design and application of AMDI for on-line detection with mass spectrometry and ion mobility spectrometry.

Keywords: ambient metastable-induced desorption ionization, ion source, ionization efficiency, FAIMS

PACS: *52.20.Hv, 51.50.+v, 82.33.Xj*

DOI: 10.1088/1009-0630/17/12/12

(Some figures may appear in colour only in the online journal)

1 Introduction

Ambient metastable-induced desorption ionization (AMDI) is a type of ion source for mass spectrometry (MS) and ion mobility spectrometry (MS) that can rapidly desorb and ionize samples through Penning ionization and ion molecular reactions in open environments. AMDI generally includes direct analysis in real time (DART) [1], low-temperature plasma (LTP) [2], and dielectric barrier discharge ionization (DBDI) [3]. The advantages of the aforementioned methods include soft ionization, low ionic discrimination, little or no sample pretreatment, high throughput, and rapid and noncontact analysis, among others [4]. Because of their advantages, these ionization methods have been widely used in on-line MS and IMS for surface analysis, authenticity identification, fingerprinting, pesticide monitoring on vegetables, screening for explosives and warfare agents, and drug detection on luggage, clothes, and bank notes [5].

The process of sample ionization by AMDI is typically extremely complicated. Ionization does not occur in any atmospheric pressure ion source through a single, clear mechanism, such as electron ionization (EI) [6]. Rather, a complex series of competing reactions can occur, which include gas discharge, Penning ionization [7], proton transfer and electron trapping [8].

AMDI is a metastable-induced ambient chemical ionization source. The discharge gas (typically helium, argon, or nitrogen [9]) primarily produces the excited state metastable particles in the discharge region with high voltage (usually a kilohertz sinusoidal AC power or a pulsed DC power [10]). For DART, Cody et al. suggested a mechanism in which the gas stream of excited-state helium (2^3S, 19.8 eV) induces Penning ionization of atmospheric moisture upon exiting into the

*supported by National Natural Science Foundation of China (No. 61374016), the Changzhou Science and Technology Support Program, China (No. CE20120081) and the External Cooperation Program of Chinese Academy of Sciences (No. GJHZ1218)

open environment, providing protonated water clusters (Eq. (2)). Subsequently, the $[M+H]^+$ is formed when the proton affinity of the sample M is higher than that of the ionized water clusters (Eq. (3)). Using helium as the discharge gas, this process can be summarized as follows [11]:

$$He(1^1S) + \text{energy} \rightarrow He(2^3S) \quad (1)$$

$$He(2^3S) + nH_2O \rightarrow [(H_2O)_{n-1} + H]^+ + OH^- + He(1^1S) \quad (2)$$

$$[(H_2O)_n + H]^+ + M \rightarrow [M + H]^+ + nH_2O \quad (3)$$

However, other reactions may occur as well. The outcome depends on factors such as the presence or absence of solvents or trace contaminants, temperature, gas flow rate, pressure, and electrical potentials [11]. The mechanisms involved in the formation of the molecular ions and other odd-electron species in the AMDI ion source are not fully understood.

The abundance of odd-electron ions from given analytes may directly correlate with the abundance of $O_2^{+\cdot}$ in the background mass spectrum [11]. This suggests that charge-exchange may play a role, as shown in the following reaction sequence, where M donates an analyte molecule that possesses an ionization energy (IE) less than the IE of diatomic oxygen (12.07 eV):

$$He^* + O_2 \rightarrow O_2^+ + e^- + He \quad (4)$$

$$O_2^+ \cdot + M \rightarrow M^+ \cdot + O_2 \quad (5)$$

$$O_2^+ \cdot + M \rightarrow \text{fragment}^+ + O_2 + R \quad (6)$$

(IE of M< 12.07 eV)

The presence of N_2^+ is also defined in ambient air, which is produced from the reaction between metastable He and N_2 due to Penning ionization [12].

$$He^* + N_2 \rightarrow He + N_2^+ + e^- \quad (7)$$

The ion source efficiency, namely, the initial abundance of $[M+H]^+$, is directly related to the sensitivity of MS and IMS. In 2007, Na Na et al. briefly investigated the effects of discharge power and gas flow rate of DBDI and found that the discharge power leads to a significant gain in the signal intensity before breakdown and that the highest signal-to-noise ratio can be achieved at a flow rate of 35 m/s [4]. In 2009, Harris et al. presented the first experimentally validated finite element simulations of an ambient DART-type plasma-based (metastable-induced) chemical ionization source [13]. Nevertheless, recent studies focused on the profit matrix [14] or the placement method and positioning of the sample [15], which are sorts of brief sample pretreatments, but these studies have not focused on the physical mechanism that affects the efficiency. Related to Eqs. (1) to (3), these groups primarily studied the characteristics of sample M without the concentrations of $He(2^3S)$ and H_2O, which are crucial to the investigation of the ionization efficiency. Therefore, it is imperative to determine the optimal discharge parameters for a stable and efficient ionization to obtain an appropriate combination with FAIMS.

The objective of the present work is to explore the influence and significance of key discharge parameters [16] on the efficiency and stability of AMDI. A home-made FAIMS instrument was selected as the ion abundance detector, which has the advantage of low ion loss. Helium was selected as the discharge gas because of its merit of a high yield and utilization ratio of protons and hydrated protons. Acetone was selected as the ionization sample because the high energy of proton affinity ensures that the primary signal is acetone rather than other molecules, such as $[(H_2O)_{n-1}+H]^+$, $O_2^+\cdot$ and N_2^+, which have lower proton affinities, as shown in Table 1. The main discharge parameters investigated in this study include discharge power, discharge frequency, gas flow rate and structure. Other factors, such as the exact positioning, distance, and angle of AMDI with respect to the sample surface and the FAIMS, which are not critical [1], will be specifically discussed in a future study. The influence mechanism is discussed by considering the discharge mode transformation, micro turbulence, proton transfer, electron trapping and ion diffusion. The results are pertinent to the design of AMDI, which aims to obtain highly efficient and stable sample ions.

Table 1. The ionization energies, electron affinities and proton affinities of H_2O, O_2, N_2 and acetone

Name	Ionization energy (eV)	Electron affinity (eV)	Proton affinity (eV)
Water	12.62	-	7.158
Oxygen	12.07	0.448	4.363
Nitrogen	15.58	-	5.116
Acetone	9.40	0.00152	8.407

2 Experimental setup

2.1 Instrumentation

Experiments were performed using two instruments: a home-made FAIMS and a home-made AMDI interfaced to the FAIMS. As shown in Fig. 1, the AMDI is primarily composed of a tungsten needle electrode, a bundle electrode, a quartz dielectric tube, a heater wire and a piece of grid electrode. The grounded grid electrode acts as an ion absorber, and it serves to remove ions of opposite polarity from the discharge region. Hence, the output of pure metastable helium will not interfere with reactions in the ionization region, thereby preventing signal loss from ion-ion recombination.

The bundle electrode and the heater wire are wrapped around the quartz dielectric tube. The tube has a length of 100 mm and inner diameter of 3 mm.

An AC power of 10 kHz was applied between the bundle electrode and the tungsten needle. The gas temperature can be adjusted from room temperature up to 700 K.

The dimensions of the FAIMS mobility region are 15 mm (length) × 10 mm with a vertical height of 0.5 mm, and the voltage parameters are as follows: RF (radio frequency) field amplitude of 30000 V/cm, frequency of 1 MHz, duty cycle of 30%, and CV (compensation voltage) scan range of ±30 V. The gas flow rate range is 9-11 m/s.

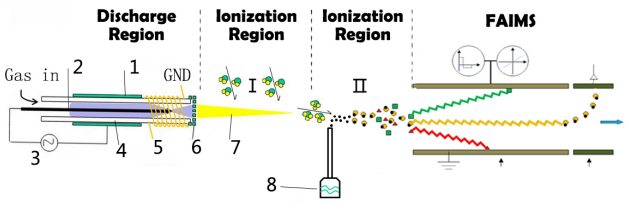

Fig.1 Schematic of the sample detection process by AMDI-FAIMS. 1 Bundle electrode, 2 Needle electrode, 3 Alternating voltage, 4 Quartz dielectric tube, 5 Heater wire, 6 Grid electrode, 7 Pure metastable particles, 8 Sample. I The process of Eq. (2), II The process of Eq. (3)

2.2 Discharge parameters and sample

Helium (99.999%) from the Shangyuan Gas Corporation (Nanjing, China) was used as the discharge gas. Acetone with a purity of 99 % was purchased from Sinopharm Chemical Reagent Co., Ltd. Fig. 2 shows the singlet of acetone that was detected by FAIMS at an ionization discharge of 3.8 kV and a flow rate of 5.3 m/s.

Experimental alternating voltages of 0-3.5 kV at frequencies of 0-10.5 kHz were applied for AMDI. The gas flow rate of helium can range from 0 m/s to 20 m/s. The room temperature was 20 °C with a relative humidity from 50 % to 60 %. A sufficient amount of acetone, within 1.88 ppm, was used.

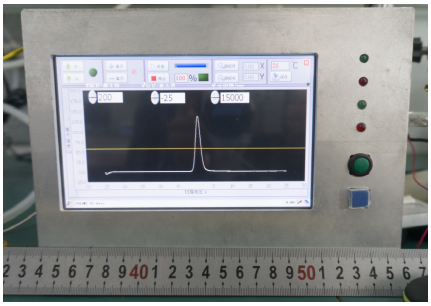

Fig.2 FAIMS spectrum of acetone

3 Results and discussion

3.1 The effects of the discharge power and frequency on the ionization efficiency

As previously mentioned, the processes described in Eqs. (1) to (3) indicate that as the concentration of produced He(2^3S) atoms increases, the number of water clusters that are protonated increases. Because of the long lifetime of the helium 2^3S state, the concentration of metastable helium atoms is primarily determined by the discharge power. The effects of the discharge power on the ion abundance are shown in Fig. 3(a) and Fig. 3(b).

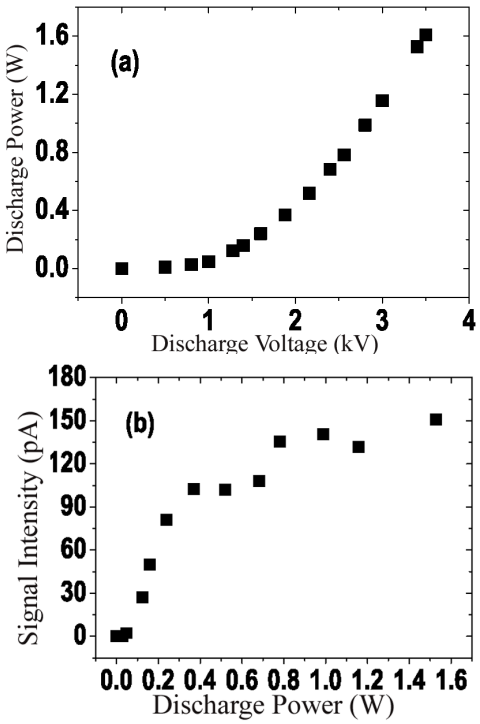

Fig.3 Voltage-vs-power (a) and power-vs-signal intensity curves (b) for the ambient metastable-induced desorption ionization

The curve in Fig. 3(b) shows that the signal rapidly increases as the discharge power increases from 0.1 W to 0.4 W. Then, the signal gradually increases to saturation at approximately 140 pA from a power of 0.8-1.6 W. Further increasing the discharge power may result in breakdown of AMDI. According to ion recombination theory, the main recombination process in the atmosphere is ion-ion recombination, which is described by Eqs. (8)-(9) [17] below, where α is a recombination coefficient, n is the initial ion concentration and n_t is the concentration at time t.

$$n_t = n/(1 + n_0 \alpha t). \tag{8}$$

Therefore, the final ion current of acetone is

$$I = n_t Q \eta. \tag{9}$$

Here Q is the gas flow rate and η is the ratio of proton transfer from $(H_2O)_nH^+$ to acetone.

The ion traveling time from the AMDI output to the ion current detection electrodes is approximately 10 ms, the recombination coefficient of $(H_2O)_nH^+$ in the atmosphere is approximately 10^{-6} cm^3/s, the flow rate is 2.4 L·min^{-1} and η is approximately 20% in the atmosphere. In this case, the dependence of the ion

current of acetone on n can be estimated and the result is shown in Fig. 4

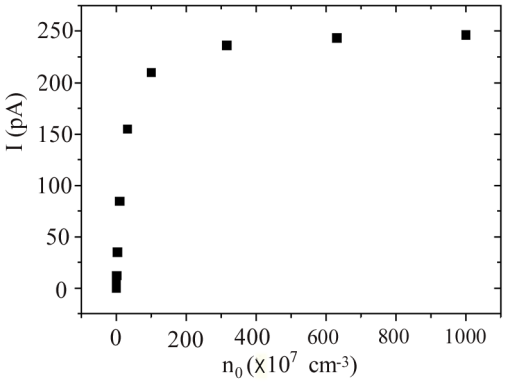

Fig.4 Ion current of acetone on n_0

As shown in Fig. 3(b) and Fig. 4, the estimated trend-line is in good agreement with the experimental results, which indicates that the ionization efficiency of AMDI is limited by ion-ion recombination, and the maximum signal intensity is approximately 100 pA for a discharge power of approximately 1 W. This result provides an experimental foundation for the selection of appropriate discharge power.

The effect of the discharge frequency was investigated in this study by increasing the frequency from 6.0 kHz to 10.5 kHz while maintaining the power at 6 W. As shown in Fig. 5, the sample current fluctuates from 31.49 pA to 37.07 pA. Compared to the power-vs-frequency curve shown in the inset (in Fig. 5), it is clear that this fluctuation, to a great extent, resulted from the small change in the discharge power. Higher and lower frequencies may change it into an unexpected discharge mode, such as the breakdown and the disappearance of plasma, respectively.

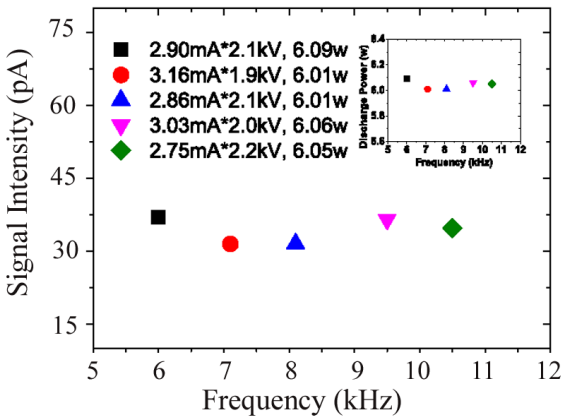

Fig.5 The effect of the frequency on the steady discharge power. The inset shows the original data source of power and frequency

3.2 The effect of the discharge gas flow rate on the ionization efficiency

The ion current of acetone as a function of the gas flow rate is shown in Fig. 6 for a constant discharge power of 0.9 W.

When the gas velocity is less than 9.0 m/s, the quantity of metastable helium particles (2^3S, 19.8 eV) increases as the flow rate increases. High-energy metastable particles are easier to diffuse and react through collisions with other particles in this range of gas flow rates, thereby producing more sample ions. In addition, a higher gas flow rate provides more ions into the FAIMS because the sample ion has a lower recombination rate at higher speed. The linearity of 0.9986 (Fig. 7(a)) clearly indicates that the ion current has a linear correlation with the gas flow rate, which is in excellent agreement with Eq. (9).

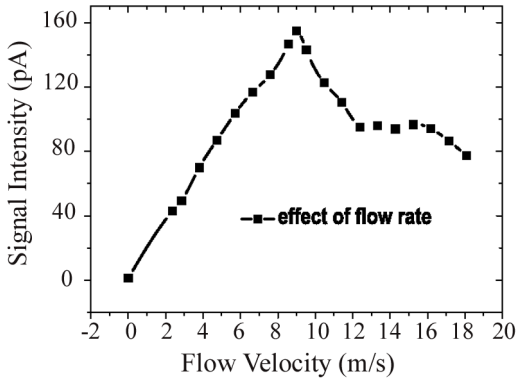

Fig.6 Effect of the flow rate on the signal intensity under steady power

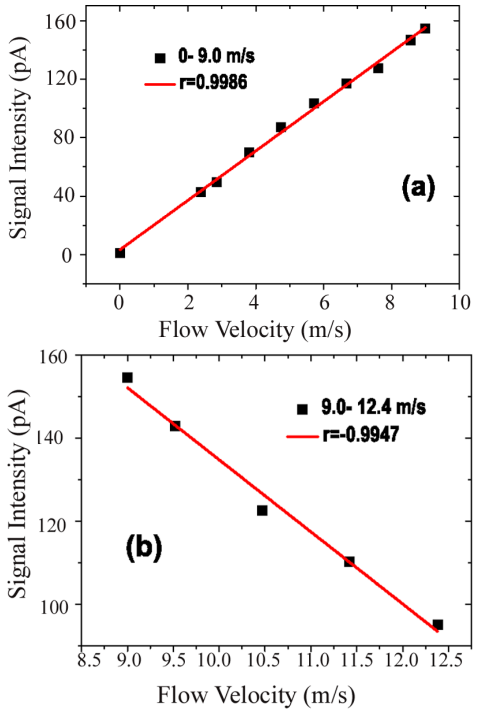

Fig.7 Data fitting of 0-9.0 m/s (a) and 9.0-12.4 m/s (b)

When the primary particle flow rate is greater than 9.0 m/s, i.e., the sample has been sufficiently ionized, the discharge gas flow rate reaches the flow rate of FAIMS. A higher discharge gas flow rate cannot draw a higher concentration of ions into FAIMS. In contrast, the FAIMS orifice functions as a gas restrictor, which blocks the entrance of extra ions into FAIMS and leads

to further recombination of sample ions. Thus, the signal intensity decreases as the discharge gas flow rate increases from 9.0 m/s to 12.4 m/s, as indicated by the negative linear attenuation of 0.9947 in Fig. 7(b). The flat curve between 12.4 m/s and 16.2 m/s indicates the occurrence of turbulence after the flow rate gets greater than 12.4 m/s. The turbulence will increase particle collisions and promote ion production. However, when the flow rate is greater than 16.2 m/s, the decreasing effect of the gas flow is more prominent than the promoting effect of the turbulence. A better understanding of the mechanisms involved in atmospheric reactions may offer explanations for the above phenomena.

3.3 Electromagnetic interference

AMDI emits considerable interference into FAIMS chips, though there are several safeguards around the FAIMS's weak-current detector to protect the signal performance from electromagnetic radiation spread through space. In this case, we investigate the relationship between the properties of the grid and the signal performance (Fig. 8): the measurement without the grid is unable to detect weak signals because the interference increases to 50 pA (with a standard deviation of 10.60). Placing a single grounded grid can reduce the interference to less than 5 pA (with a standard deviation of 1.40). Sets of stacked mesh grids can reduce the signal noise level to below 10 fA.

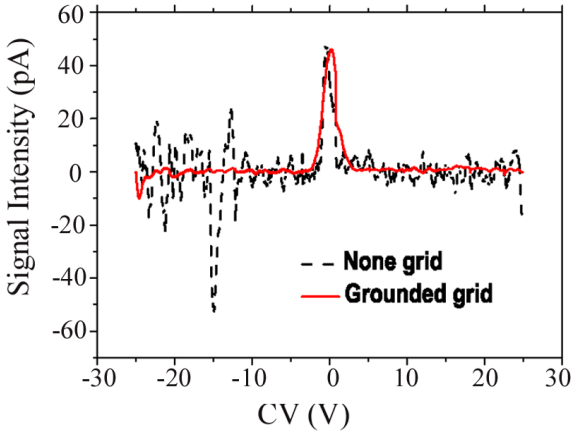

Fig.8 The interference with and without a grounded grid

4 Conclusions

Ambient metastable-induced desorption ionization has a number of advantages, such as soft ionization, simplified or no sample pre-treatment, low ionic discrimination, high throughput and high ionization efficiency. This method plays an increasingly important role compared to traditional ionization methods and is widely used in ion mobility spectrometry and mass spectrometry. We constructed an ambient metastable-induced desorption ionization source to explore an optimal balance among flow rate, discharge power, frequency and other electric field parameters that lead to steady, high-efficiency desorption ionization. The discharge power and the flow rate both have optimal values for the ionization efficiency. The structure and material, particularly a grounded grid, can reduce ion recombination and enhance signal performance.

However, the results apply only to an experimental device based on the mechanism of Penning ionization and proton transfer. To accurately understand the reactions between ions, other ambient air particles should be considered in these reactions, particularly in some specific environments, such as chemical factories, mine tunnels, and drug crime scenes. Optimizing the preparation parameters for the specific sample [18], improving the structure, selecting a quality dielectric material and determining how to control the reaction of three-body collisions require follow-up work and in-depth study.

References

1 Cody R B, Laramee J A and Durst H D. 2005, Anal. Chem., 77: 2297
2 Harper J D, Charipar N A, Mulligan C C, et al. 2008, Anal. Chem., 80: 9097
3 Na N, Zhao M X, Zhang S C, et al. 2007, J. Am. Soc. Mass. Spectr., 18: 1859
4 Na N, Zhang C, Zhao M X, et al. 2007, J. Mass Spectrom., 42: 1079
5 Osuga J and Konuma K. 2011, Journal of Synthetic Organic Chemistry Japan, 69: 171
6 Dempster A. 1918, Physical Review, 11: 316
7 Jin D, Yang Z, Xiao K, et al. 2009, Plasma Sci. & Technol., 11: 48
8 Gross J H. 2014, Anal. Bioanal. Chem., 406: 63
9 Jorabchi K, Hanold K and Syage J. 2013, Anal. Bioanal. Chem., 405: 7011
10 Lu X, Laroussi M and Puech V. 2012, Plasma Sources Sci. Tech., 21: 034005
11 Cody R B. 2009, Anal. Chem., 81: 1101
12 Zhu W C, Li Q, Zhu X M, et al. 2009, Journal of Physics D: Applied Physics, 42: 202002
13 Harris G A and Fernandez F M. 2009, Anal. Chem., 81: 322
14 Song L, Gibson S C, Bhandari D, et al. 2009, Anal. Chem., 81: 10080
15 Musah R A, Cody R B, Dane A J, et al. 2012, Rapid Commun. Mass. Sp., 26: 1039
16 Chen Ran, Chen Chilai, Kong Deyi, et al. 2013, Plasma Sci. Technol., 15: 845
17 Lehtipalo K, Sipila M, Riipinen I, et al. 2009, Atmos. Chem. Phys., 9: 4177
18 Wang Y, Li C, Huang L, et al. 2014, Anal. Chim. Acta, 845: 70

(Manuscript received 21 November 2014)
(Manuscript accepted 20 April 2015)
E-mail address of corresponding author
CHEN Chilai: chlchen@iim.ac.cn